THE GEOMETRIC CORRECTION PROCEDURE USING TOPOGRAPHIC MAP VERSUS GPS-DERIVED GROUND CONTROL POINTS FOR LULC ANALYSIS

Muhammad Yazrin Yasin (1)(2), Norzailawati Mohd Noor (3), Mariney Mohd Yusoff (1), Jamalunlaili Abdullah (2)

[1] Department of Geography, University of Malaya, 50603 Kuala Lumpur

[2] Faculty of Architecture, Survey and Planning, University of Technology MARA, 40450 Shah Alam, Selangor

[3]Kuliyyah of Architecture and Environmental Design, International Islamic University of Malaysia, 50728 Kuala Lumpur

Email: yazrinyasin@gmail.com; norzailawati@iium.edu.my; mariney@um.edu.my; jamal858@uitm.edu.my

ABSTRACT: Precision measurement of land use land cover change detection is essential for urban growth assessment. Remote sensing imagery provide an integrated monitoring of the temporal changes of urban growth. Accurate geometric correction relies largely on accurate rectification of the remotely sensed data to produce classified thematic changes maps. The study utilised data from Landsat 5, 7 and 8. The rectification process involves two sources of references which are the digitized topographic map and the ground control points acquired using Global Positioning System (GPS). The study attempts to compare which sources produce higher rectification accuracy. Topographic map is acquired from the Department of Survey and Mapping Malaysia with 1:10,000 scale, 5 meters contour line and rectified skew orthomorphic grid projection. Ground truthing utilised Android 10.36.0 GPS WGS84 capability smartphone. The study found the ground control points acquired using smartphone with GPS capability were much more accurate to those acquired from topographic maps. Root-mean-square error (RMSe) of the GPS-derived control point, source point and correction point show higher accuracy results acquired from ground truthing.

Keywords: Geometric correction, ground control points, ground truthing, root-mean-square error.

INTRODUCTION

With rapid economic and urban growth, land resources have become substantial, carrying significant sustainable development implications. Land use land cover (LULC) change has been much debated topic and a major research attempt among urban planners, and predictions of major environmental changes in the future are increasing (Viana *et al*., 2019). Incorporating land use land cover change detection and satellite imagery exemplifies the most effective and efficient technology for developing national, regional and urban physical development in the course of time (Noszczyk 2018).

Nevertheless, satellite imagery has inevitably associate with certain degree of errors. The errors are possibly caused by the selection of the classification system, atmospheric condition, quality and ability of sensors, and last but not least is the rectification accuracy. During LULC change analysis of two same region of interest acquired in two different dates, a confusion on rectification error may arise as change, while it isn't (Smith and Atkinson, 2001). This show some analysts tend not to focus on frequently disregard issues of how rectification process could compromise LULC change analysis by not choosing the appropriate technique. The rectification processes involve identifiable attributes (object-based) position verification in both satellite imagery and a corresponding map coordinate system (Wang and Li, 2019). The *x* and *y* position value of object in the image together with its position in the map coordinate system (latitude, longitude) are determined. These attributes are referred as ground control points (GCPs) and are used for geometric transformation, a common operation in geometric correction procedure. A geometric transformation also known as coordinate transformation assigns satellite imagery into projection-based map coordinate system so that the image can be relate with its real-world location.

GCPs conventionally are produce through map coordinates, usually topographic maps that are endorsed by the national department of survey and mapping. However, GCPs are also produce through ground-truthing, using a portable GPS-enable device, such as smartphone. A study on coastal monitoring by Kim *et al*., (2013) has proved higher accuracy of using smartphone image triangulation compares to conventional survey mapping to produce GCPs. Another study by Alsubaie *et al*., (2017) presented a new method that expedite the use of smartphones as a portable GPS-enable devise for mobile mapping system. USGS has claims GPS nominal accuracy is <5-meter RMS with 95% confidence interval. These show smartphones are becoming highly advance piece of technology and are rapidly closing the gaps between computers and other based navigation sensors. Therefore, this study attempts to compare which reference sources produce higher rectification accuracy.

Study Area

The study area is Sepang, Selangor, Malaysia located at 2°45'38"N and 101°44'15"E with a total coverage of 56,150 km^2 and the main land cover consists of urban built-up areas, vegetation and open spaces. The population in 1995 is 90,000 and leaped to 189,9000 in 2015 (Statistical Department of Malaysia, 2018). Sepang enjoys tropical weather year around with quiet humid atmosphere due to its proximity to Malacca Straits, temperatures range from 26° to 36°. Cloud coverage is rather high and wettest month is November though it does experience occasional rainfall. The study area was largely and rapidly growing from 1995 to 2015 with rapid land use changes because it is part of vibrant Greater Kuala Lumpur and proximity to Putrajaya (Yasin *et al*., 2019)

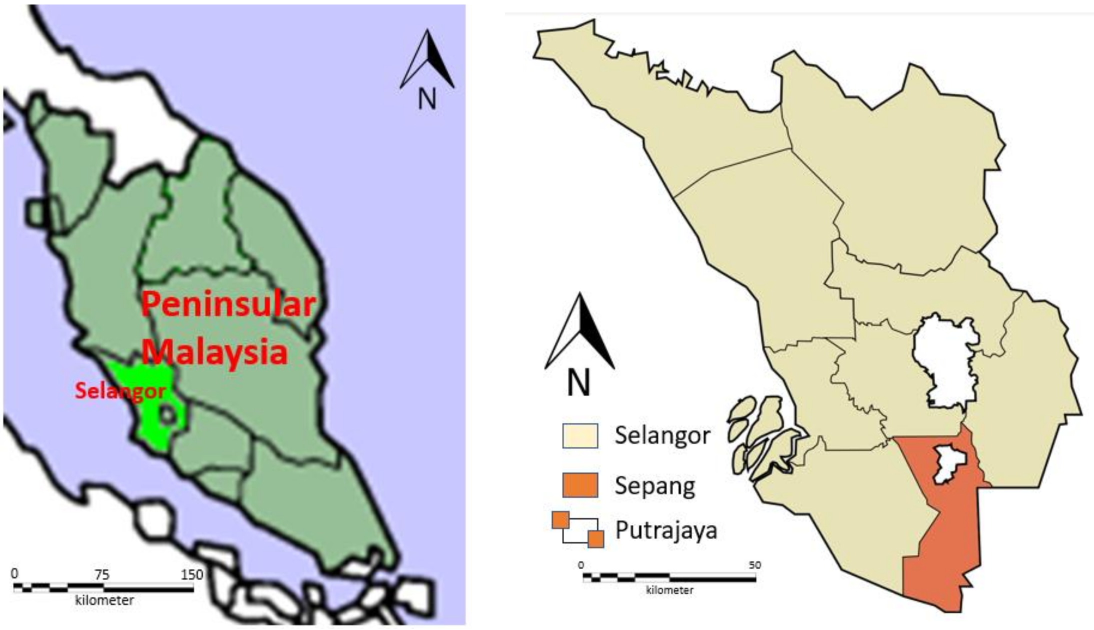

Figure 1. Map of state of Selangor in Peninsular Malaysia (left) and Sepang in state of Selangor

DATA SETS AND MATERIAL

The primary data are consisting of the remote sensing imagery, topographic map and GPS derived ground control points. The remote sensing imagery is the currency of remote sensing method for change detection and analysis. Two types of remote sensing imagery acquired for the study are Landsat (MSS and OLI-TRIS). The spatial resolution for each imagery is 30-meter. Topographic map is a feature map consist of highways, roads, railways, building, vegetation and boundaries. Highways and roads appeared as dual and single carriageways. Boundaries are hierarchical – international, state, district, mukim and reserve. Vegetation and built up areas represent by symbols. The GPS-derived GCPs is a satellite based global positioning technology provides correctly coordinates of ground reference acquired through ground truthing.

Table 1 Primary data

Type of data	Specification	Sources
Landsat TM	1990 – 1998 30 meters resolution 7 bands	USGS Landsat Data Access
Landsat ETM +	2000 – 2012 30 meters resolution 8 bands	USGS Landsat Data Access
Landsat 8 OLI-TIRS	2014-2018 30 meters resolution 11 bands	USGS Landsat Data Access
Topographic map	Scale 1:10,000 25 meters contour line Projection: Rectified Skew Orthomorphic Grid	Department of Survey and Mapping Klang Valley Series no. DNMM6101
GPS-derived GCPs	Android 10.36.0 WGS84	Ground truthing

United State Geological Survey (USGS) through Landsat Data Access provide data products held in USGS archives can be searched and downloaded free of charge from several sources. Landsat mission has been launched since 1972 to deliver high quality, global data on Earth's surfs. Department of Survey and Mapping Malaysia provide various services related to mapping, cadastre, and geodetic with reasonable fees. Details of remote sensing imagery acquired for this study is as Table 2.

Table 2 Primary remote sensing imagery acquired

Sensors	Month/day	Year	Spatial resolution (m)	Time	Path/row	Band combination
Landsat 5	12/27	1990	30m	10.30am	127/58	1,2,3,4,7
	11/25	1992		11.15am	126/58	
	11/28	1994		10.27am	127/58	
	06/26	1996		10.47am	127/58	
	02/08	1998		10.39am	126/58	
	03/17	2000		11.06am	127/58	
Landsat 7	05/02	2002		10.18am	127/58	
	12/23	2004		10.48am	126/58	
	03/02	2006		11.49am	126/58	
	07/29	2008		10.42am	127/58	
	01/02	2010		10.25am	127/58	
	06/04	2012		10.29am	127/58	
Landsat 8	03/24	2014		10.18am	127/58	2,3,4,5,7
	03/29	2016		11.13am	127/58	
	04/04	2018		10.30am	127/58	

The study acquired 15 Landsat imagery varied between year 1990 and 2018 in every other year. The Landsat imagery come with different sensors capability with Landsat 5 equipped with both the Multi-Spectral Scanner (MSS) and the Thematic Mapper (TM). It is equipped with seven bands and one thermal infrared band (band). Landsat 7 equipped with Enhanced Thematic Mapper Plus (ETM +) with 8 bands, band 6 thermal infrared and band 8 panchromatic 15 meters resolution. Last is Landsat 8 equipped with Operational Land manager (OLI) and Thermal Infrared Sensor (TIRS) with two thermal infrared bands, band 10 and 11, one panchromatic band 8.

METHODS

Ground-truthing

The study has conducted a ground truthing was conducted to generate GPS-derived GCPs for reference data. The 15 well distributed GPS-derived GCPs that was generated to register all the imagery using a second-degree polynomial model are shown in Figure 1 below. The use of 10 GCPs (5 were reserved for accuracy verification) shown by location icon did result in absolute accuracy of 2 – 4 meters (1 – 2 pixels). The GCPs was cautiously generated in the centre of the conflict point of T-Junction, cross intersection, different level intersection, roundabout, or viaduct to get attainable accuracy.

Figure 1. GPS-derived Ground Control Points of the study area

Table 3. GPS-derived Ground Control Points Longitude – Latitude of the study area

No.	Longitude – Latitude	Description
1.	2°38'16.7"N 101°37'27.4"E 2.637974, 101.624269	Junction Kg Ulu Tris – Federal Road 5
2.	2°38'29.7"N 101°42'55.4"E 2.641569, 101.715391	Intersection Kg Sg Pelek – Federal Road 5
3.	2°41'27.3"N 101°45'06.9"E 2.690904, 101.751907	Intersection B48 state road Federal Road 5 Pekan Sepang
4.	2°44'23.5"N 101°45'21.9"E 2.739868, 101.756087	Intersection B48 and 1266 to Enstek
5.	2°45'55.4"N 101°45'07.2"E 2.765400, 101.752011	Intersection B48 – 344 Jalan Kuarters KLIA
6.	2°43'36.8"N 101°43'36.5"E 2.726890, 101.726809	Roundabout Jalan KLIA S3 - 27 to KLIA cargo terminal
7.	2°45'24.7"N 101°41'57.6"E 2.756870, 101.699322	T Junction Jalan KLIA 1- 182-26 to KLIA long term car park
8.	2°48'19.6"N 101°44'47.9"E 2.805452, 101.746636	Viaduct 32 - B48 to Sepang Land Office
9.	2°49'26.8"N 101°41'37.0"E 2.824114, 101.693614	Viaduct 29 – Jalan Kota Warisan
10.	2°53'39.9"N 101°39'30.0"E 2.894413, 101.658338	Intersection 29 – 30 Persiaran Selatan Cyberjaya
11.	2°53'18.0"N 101°44'11.4"E 2.888321, 101.736508	Intersection B48 - B18 Jenderam Hilir
12.	2°53'47.7"N 101°40'40.5"E 2.896588, 101.677907	T-Junction Persiaran Perdana – Lebuh Gemilang to PICC
13.	2°55'41.7"N 101°39'57.4"E 2.928245, 101.665934	Viaduct Lingkaran Putrajaya E6 – 29 to Cyberjaya
14.	2°56'34.0"N101°44'50.3"E 2.942768, 101.747313	Intersection B13 - Jalan Aman/ Jalan Maktab Kg Sg Merab
15.	2°58'16.8"N 101°43'11.3"E 2.971323, 101.719803	Viaduct E26 – Persiaran Putrajaya

Geometric correction

The pre-processing of Landsat imagery was carefully performed to correct for any distortion due to the qualities of sensors, multitemporal (dates) data and atmospheric conditions. Landsat imagery have been projected into Universal Transverse Mercator (UTM) map coordinates by USGS. This method determined the reassigned 'synthetic' pixel values through estimating block pixels of the original image matrix encircling the output pixel.

Landsat imagery were later converted to Latitude-Longitude format for displaying cartographic view. Other maps (Selangor state map and district boundary map) are also registered to Lat-Long. Price and Usery (1984) suggest the polynomial mapping are represents by:

$$\mathrm{UTM} = c_0 + c_1x + c_2y + c_3x^2 + c_4xy + c_5y^2 + c_6x^3 + c_7x^2y + c_8xy^2 + c_9y^3 \qquad \text{Eq. 1}$$

where GCPs values of *x* and *y* are the recognized image coordinates in pixel and scanline coordinates

A dense network of GCPs on both topographic map and Landsat imagery must be accurately detected and located. Attributes location of the GCPs were identified using Envi version 4.0 interactive image processing system in pixel and coordinates. Low spatial resolution could jeopardise identifying attributes as GCPs usually being the centre of the conflict point of intersections (T-Junction, cross intersection, different level intersection, roundabout, or viaduct). In this scenario, pixel refinements are performed, determining image coordinates to ±1 data pixel equivalent to ±30m for Landsat TM and ETM+.

To register the scene and decrease the RMS errors, the study select both the 1:10,000 scale Klang Valley topographic map, and 15 well-distributed geographic GCPs acquired and measured in the ground truthing using an Android 10.36.0 WGS84 compatible device to be used for the geometric transformation. These GCPS are mostly pinpoint to road intersections in the study area to ensure they are clearly visible in both source points (remote sensing imagery) and reference point (GCPs and topographic map). A uniformly distributed and a minimum, a medium, and a maximum number of reference point (in the range of five to 15 points) were used for each data set, in order to investigate the optimum number of reference point required (Tonkin and Midgley, 2016). For example, although the study acquired 15 GCPs, some datasets require different numbers of GCPs between 5, 10 and 15 to get optimum result.

A second-order polynomial is applied because it is uniformly distributing the least-squares solution throughout the image (Zhao *et al.*, 2016). For onscreen pinpoint, infrared band of the Landsat TM and ETM + was the most suitable, due to high contrast between built up areas and vegetation. For Landsat OLI-TIRS, the false composite image (green, red and near infrared) is the most suitable combination because it has maximum contrast between built up, vegetation and waterbody feature.

RESULTS AND DISCUSSIONS

To check the relative accuracy of the control point, source point and correction point, the study use format rectification accuracies of RMSE_{xy} of ±1.34 to ± 0.15 data pixel for both full and subscene areas using second order polynomials in the study area. A slight variation or the RMSE_{xy} in the geometry was detected for all the Landsat TM, Landsat ETM+, and Landsat OLI-TRIS imagery due to multitemporal observations. The study uses 15 satellite imagery between 1990 and 2018, which was 28 years of urban growth observations where rapid development take place. Analysis of Landsat TM shows that GPS-derived errors of approximately ±0.40 compares to ±0.49 map-derived errors. Landsat ETM+ also shows that GPS-derived errors of ±1.14 compares to ±1.34 map-derived errors. Landsat OLI-TIRS however show the least differences between GPS-derived errors of approximately ±0.53 with map-derived errors of approximately ±0.55. Thus, the findings of overall results dataset are better off with GPS-derived GCPs than the topographic map.

Table 4. The Root-Mean-Square error ($RMSE_{xy}$) of the control point, source point and correction point using GPS-derived GCPs and topographic map 1:10,000 scale

Reference point	imagery	No.	control point $RMSE_{xy}$	source point $RMSE_{xy}$	correction point $RMSE_{xy}$
GPS-derived GCPs	Landsat TM	5	± 0.15	± 0.52	± 0.45
		10	± 0.26	± 0.46	± 0.41
		15	± 0.32	± 0.45	± 0.40
	Landsat ETM +	5	± 0.84	± 1.31	± 1.24
		10	± 0.90	± 1.26	± 1.15
		15	± 0.98	± 1.26	± 1.14
	Landsat OLI-TIRS	5	± 0.42	± 0.65	± 0.53
		10	± 0.45	± 0.63	± 0.54
		15	± 0.49	± 0.63	± 0.56
Topographic map	Landsat TM	5	± 0.37	± 0.56	± 0.53
		10	± 0.44	± 0.55	± 0.51
		15	± 0.49	± 0.49	± 0.49
	Landsat ETM +	5	± 0.83	± 1.40	± 1.34
		10	± 1.06	± 1.38	± 1.30
		15	± 1.16	± 1.28	± 1.23
	Landsat OLI-TIRS	5	± 0.41	± 0.70	± 0.55
		10	± 0.53	± 0.69	± 0.65
		15	± 0.58	± 0.64	± 0.63

Analysis of Landsat TM revealed that errors of approximately ±0.45 can be reduced to ±0.40 by using higher GCPs. Landsat ETM+ also revealed that errors of approximately ±1.24 can be reduced to ±1.14 using the same amount of GCPs. However, Landsat OLI-TIRS shows error approximately ±0.53 using the least GCPs. Thus, Landsat OLI-TIRS dataset was best reduced RMS error with minimum number (5) of GCPs, while Landsat TM and Landsat ETM + with maximum number (15) of GCPs. The findings also showed significant differences in absolute locational between the corrections applied to all the above dataset. However, the result also proved the geometric correction accuracy was not always improved by increasing the number of GCPs. Also, important to be noted, although ETM+ dataset has higher value of RME error, but the actual ground distance is not very difference. For example, the RMS error of TM and OLI-TIRS has only 2 meters error lower than the Landsat ETM+ dataset on the ground.

CONCLUSIONS

All GPS-derived GCPs in ground-truthing produced higher accuracy than topographic map derived GCPs on geometric correction procedure. However, the differences are less than a meter. This is because the highest GPS nominal accuracy is 4-meter RMS (95% confidence interval), higher than the coarse resolution of Landsat TM, ETM+ and OLI-TIRS. Geometric transformation or coordinate transformation on LULC change detection with a series satellite images would result an amount of errors especially involve rapid changes of land cover classification. The study area was vastly growing from 1995 to 2015 with rapid land use changes. However, the study uses 15 two-year interval Landsat imagery, thus the rapid changes between intervals are not so obvious. Nevertheless, the study suggests LULC change detection should define a set of GCPs, decide upon an approach for map derived GCPs coordinates, and quality control of geometric correction procedure.

References

Alsubaie, N. M., Youssef, A. A., & El-Sheimy, N. (2017). Improving the Accuracy of Direct Geo-Referencing of Smartphone-Based Mobile Mapping Systems Using Relative Orientation and Scene Geometric Constraints. *Sensors, 17*(2237).

Department of Statistics Malaysia. (2018). *Statistical Handbook Malaysia 2018*.

Kim, J., Lee, S., Ahn, H., Seo, D., Seo, D., Lee, J., & Choi, C. (2013). Accuracy evaluation of a smartphone-based technology for coastal monitoring. *Measurement, 48*, 233-248.

Noszczyk, T. (2018). A review of approaches to land use changes modelling. *Human and Ecological Risk Assessment: An International Journal*.

Price, J. C., & Usery, E. L. (1984). Cartographic Accuracy of LANDSAT-4 MSS and TM Image Data. *IEEE Transactions on Geoscience and Remote Sensing, GE 22*(3).

Tonkin, T. N., & Midgley, N. G. (2016). Ground-Control Networks for Image Based Surface Reconstruction: An Investigation of Optimum Survey Designs Using UAV Derived Imagery and Structure-from-Motion Photogrammetry. *Remote Sensing, 8*(9), 786.

Viana, C. M., Oliveira, S., Oliveira, S. C., & Rocha, J. (2019). Land Use/Land Cover Change Detection and Urban Sprawl Analysis *Spatial Modeling in GIS and R for Earth and Environmental Sciences*.

Wang, Y., & Li, M. (2019). Urban impervious surface detection from remote sensing images: a review of the methods and challenges. *IEEE Geoscience and Remote Sensing Magazine*.

Yasin, M. Y., Yusoff, M. M., & Noor, N. M. (2019). Urban sprawl assessment using time series LULC and NDVI variation: a case setudy of Sepang Malaysia. *Applied Ecology and Environmental Research, 17*(3).

Zhou, G., Yue, T., Shi, Y., Zhang, R., & Huang, J. (2016). Second-Order Polynomial Equation-Based Block Adjustment for Orthorectification of DISP Imagery. *Remote Sensing, 8*(8), 680.